*Journal of Fluorescence, Vol. 14, No. 5, September 2004 (©2004)*

# Live Imaging of Glucose Homeostasis in Nuclei of COS-7 Cells

**Marcus Fehr,[1] Sylvie Lalonde,[2] David W. Ehrhardt,[1] and Wolf B. Frommer[1,3]**

*Received March 15, 2004; accepted March 15, 2004*

Measuring subcellular glucose levels deep in tissues can provide new insights into compartmentalization and specialization of glucose metabolism among different cells. As shown previously, a FRET-based glucose-sensor consisting of two GFP-variants and the *Escherichia coli* periplasmic glucose/galactose binding protein was successfully expressed in the cytosol of COS7-cells and used to determine cytosolic glucose levels. Recording cytosolic fluorescence intensities in cells located in deeper layers of tissues is often difficult due to loss of signal intensity caused by effects of other cell layers on excitation and emission light. These interfering effects may be reduced by restricting fluorophores to occupy only a fraction of the assayed tissue volume. This can be accomplished by confining fluorophores to a sub-compartment of each cell in the tissue, such as the nucleus. The glucose-sensor was targeted to nuclei of COS7-cells. To determine, whether nuclear glucose levels can be used to track cytosolic changes, nuclear glucose concentrations were quantified as the cells were challenged with external glucose over a range of 0.5 to 10 mM and compared to cytosolic levels. Internal glucose concentrations in both compartments were similar, corresponding to ~50% of the external concentration. Taken together, these results indicate that nuclear glucose levels can be used to determine cytosolic levels indirectly, permitting more reliable quantification of fluorescence intensities and providing a tool for measurements not only in cell cultures but also in tissues.

**KEY WORDS:** Nucleus; glucose; FRET; imaging.

## INTRODUCTION

Glucose metabolism and glucose levels in groups of cells and tissues forming an organ are not necessarily uniform but likely will differ even between neighboring cells. Glucose metabolism in the liver, for example, is known to be zonal [1]. Gluconeogenesis for the synthesis of glucose and glycogen is predominantly situated in the periportal zone, whereas glycolysis and glycogen synthesis from glucose are preferentially located in the perivenous zone [2,3]. A similar zonal architecture can be found in kidney, where glycolytic hexokinase activity is mainly found in distal segments, whereas gluconeogenic activity of fructose-1,6-bisphospatase dominates in the proximal tubular epithelium [4]. In plants, gradients of glucose and sucrose between parenchyma cells, companion cells and sieve elements may be involved in loading and unloading sugar in the phloem [5]. Analyzing the differences in glucose levels and metabolism in native tissue can thus contribute to a better understanding of glucose homeostasis in a number of multicellular organisms.

Until recently, technologies for monitoring subcellular levels of metabolites in living cells were unavailable.

[1] Carnegie Institution of Washington, Plant Biology, 260 Panama Street, Stanford, California 94305–4101.
[2] Zentrum für Molekularbiologie der Pflanzen, Universität Tübingen, 72076 Tübingen, Germany.
[3] To whom correspondence should be addressed. E-mail: wfrommer@stanford.edu

ABBREVIATIONS: FRET, resonance energy transfer; GFP, green fluorescent protein; YFP, yellow fluorescent protein; CFP, cyan fluorescent protein; GGBP, *E. coli* periplasmic glucose/galactose binding protein.



1053-0509/04/0900-0603/0 © 2004 Springer Science+Business Media, Inc.

To develop a flexible strategy, the hinge-twist motion of bacterial periplasmic binding proteins (PBP) was combined with the optical advantages of green fluorescent protein variants to design a novel type of nanosensor that transforms the PBP hinge-twist motion into altered fluorescence resonance energy transfer (FRET) [6–8]. PBPs constitute a large family of binding proteins with each PBP consisting of two globular domains. The binding site is located at the cleft between the domains, which engulf the substrate and undergo a hinge-twist motion [9]. PBPs were successfully employed as binding moieties for biosensors by conjugating these proteins to chemical fluorophores [10,11]. However, chemically modified proteins are not ideal for *in vivo* applications. The development of spectral variants of GFP permits modification of PBPs with genetically-encoded fluorophores. As shown recently, the FRET change between two GFP variants attached to the *E. coli* periplasmic maltose binding protein can be used to measure maltose uptake into the cytosol of individual yeast cells [6]. Similarly, ribose import and metabolism in COS7-cells were visualized using a ribose-sensor based on the *E. coli* periplasmic ribose binding protein [8]. To monitor glucose dynamics in individual cells, a glucose nanosensor (FLIPglu-170n) with a $K_d$ of ~170 nM was developed on the basis of the *E. coli* periplasmic glucose/galactose binding protein (GGBP) [7]. An affinity mutant with a $K_d$ of ~600 $\mu$M (FLIPglu-600$\mu$) was generated, which shows higher substrate specificity and binds glucose at physiological levels. Expression of FLIPglu-600$\mu$ in the cytosol of COS-7 cells showed that at external glucose concentrations between 0.5 and 10 mM free cytosolic glucose concentrations remained at approximately 50% of external levels.

To date, these sensors have been used to measure metabolites in individual cells within a cell culture monolayer. However, analyzing differences in glucose levels between neighboring cells in native tissues requires the acquisition of fluorescence intensities from several cell layers. Expression of fluorescent nanosensors in multiple cell layers introduces several new challenges for their use. First, with conventional epifluorescence optics, fluorescence from out of focus cells will contribute significantly to the signal from cells within the focal plane, thus confounding signals from multiple cells. Second, fluorophores in overlying cells will absorb a portion of the applied excitation energy, creating a shading effect that gets progressively stronger in deeper tissue. Third, with sensors that make use of FRET, emission from the donor fluorophore can be absorbed by acceptor fluorophores in overlying tissue, both attenuating and distorting the FRET signal. Fourth, scattering and refraction by overlying cells further degrades both the emission signal and excitation intensity in deeper tissue. In addition to use of confocal and multiphoton fluorescence microcopy, restriction of fluorescence to a certain portion of each cell may help to reduce these adverse effects.

Expression of GFP in nuclei of Arabidopsis roots shows that cells in multiple tissue layers can be easily visualized and discriminated due to restriction of the signal to a fraction of the image. Restricting the expression of the glucose-sensor to the nucleus reduced the fluorescent volume in COS7-cells by ~30% as compared to cytosolic expression of the nanosensor. At external glucose concentrations between 0.5 and 10 mM, both, nuclear and cytosolic glucose levels were ~50% of external supply, reflecting the nuclear pore's passive permeability for small molecules (<1 kDa) [12,13]. Thus FLIPglu-600$\mu^{nuc}$ allows us to determine cytosolic glucose levels indirectly using a nuclear nanosensor.

## EXPERIMENTAL

### FLIP$^{nuc}$ Constructs and Plasmids

The CFP-mglB-YFP chimeric genes of FLIPglu-600$\mu$ and FLIPglu-170n [7] were subcloned into the mammalian expression vectors pCMV/myc/nuc and pEF/myc/nuc (Invitrogen) using a PCR-based cloning approach. Resulting FLIPglu-600$\mu^{nuc}$ and FLIPglu-170n$^{nuc}$ carry the triple SV40 large T-antigen nuclear localization signal sequence at the C-termini.

#### *Confocal Microscopy of Arabidopsis Seedlings*

Arabidopsis seedlings were mounted on cover slips in MS medium 3 days after being germinated on the surface of MS-agar plates. Imaging was performed with a Bio-Rad MRC1024 confocal microscope using a 60× Nikon 1.2 n.a. water immersion objective, 488 nm excitation from a 15 mW KrAr laser, and a 525/35 emission filter. Excitation energy was attenuated to 3% of laser output.

#### *Cell Culture and Transfection*

COS-7 cells were grown in D-MEM with 10% fetal calf serum and 50 U/mL penicillin and streptomycin (Sigma). Cells were cultured at 37°C and 5% $CO_2$. For imaging, cells were cultured in 8-well tissue culture glass slides (BD Falcon) and transiently transfected at 50–70% confluency using Lipofectamin/Plus Reagent (Invitrogen). Transfection efficiency as determined by counting fluorescing cells was at least 30%.

*FRET Imaging*

Imaging was performed 35–40 hr after transfection on a fluorescence microscope (DM IRE 2, Leica) with a cooled CoolSnap HQ digital camera (Photometrics). Dual emission intensity ratios were simultaneously recorded using DualView with the OI-5-EM filterset (Optical Insights) and Metafluor 6.1r1 (Universal Imaging). Excitation light was attenuated to 10% of the Lambda DG4's output (Sutter Instruments). Images were acquired within the linear detection range of the camera at intervals of 20 s. Depending on expression level, exposure times varied between 0.2 and 0.5 s. Perfusion had flow rates of 2.4 mL/min in a total volume of 0.4 mL. Glucose-free DMEM (Sigma) was used to replace the growth medium before each measurement and for continuous perfusion in the absence of glucose during each measurement. Perfusion with DMEM containing the indicated concentrations was used to apply external glucose. Due to the different set up used for the acquisition of nuclear and previously published cytosolic emission intensities [7], the ratio changes of FLIPglu-600$\mu$ were greater than the ratio changes of FLIPglu-600$\mu^{nuc}$.

*Determination of Cytosolic Glucose Concentration*

Ratio changes (delta ratio) were calculated for each single cell as the difference between average ratios during perfusion with glucose and perfusion with glucose-free medium. Ratio changes of cells expressing either nanosensor were averaged. The minimum delta ratio ($\Delta R_{min}$) at complete absence of glucose and the maximum delta ratio ($\Delta R_{max}$) at saturation with glucose were obtained by non-linear regression of averaged delta ratios using Eq. (1): $\Delta r = n[glc]/(K_d + [glc]) \times (\Delta R_{max} - \Delta R_{min}) + \Delta R_{min}$, where [glc], glucose concentration; $n$, number of binding sites. To compare the results for the different nanosensors the delta ratios were normalized using Eq. (2): $S = (\Delta r - \Delta R_{min})/(\Delta_{max} - \Delta R_{min})$, where $S$, normalized delta ratio (saturation). Cytosolic glucose concentrations were obtained from normalized ratio changes

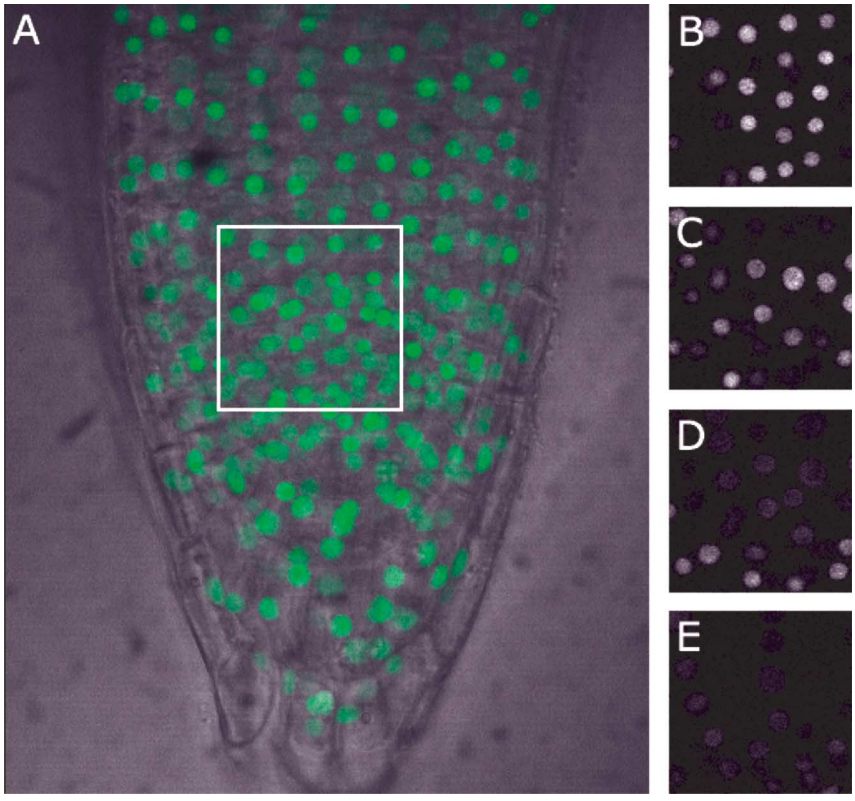


**Fig. 1.** Confocal optical sections of an Arabidopsis root tip in a transgenic plant expressing a GFP::cDNA fusion protein that localizes to the nuclear lumen [14]. (A) Brightest point projection of 21 optical sections showing labeled nuclei in multiple cell layers. A single bright field image is merged with the projection image to show the tissue context of the nuclei. (B–E) Single confocal sections from the boxed area in (A) revealing resolved nuclei in the 1st through 4th cell layers.

using Eq. (3): $[glc] = (K_d \times S)/(1 - S)$, where $[K_d]$, binding constant as determined *in vitro* [7]. To demonstrate that nuclear and cytosolic levels are ~50% of external supply a linear regression was performed on the internal concentrations when displayed as a function of external supply.

## RESULTS AND DISCUSSION

### GFP Emission from Nuclei of Arabidopsis Seedlings

To demonstrate that fluorescence from single nuclei in different tissue layers can be separated without overlaying emission, GFP was targeted to the nuclei of Arabidopsis roots. Confocal sections of nuclear GFP expression show well-discriminated fluorescence signals from individual nuclei (Fig. 1A). Although fluorescence intensity dropped significantly with the distance from the root surface, nuclear GFP-expression permitted acquisition of emission intensities in individual cells even deep in native tissues (Fig. 1B–E).

### Nuclear Expression of the Nanosensors Reduces the Fluoresecent Fraction of Transfected Cells

To direct the nanosensor to the nuclei of cultured Green African Monkey kidney derived COS-7 cells, FLIPglu-600$\mu$ was subcloned into the mammalian expression vector pEF/myc/nuc carrying the triple SV40 large T-antigen nuclear localization signal sequence (FLIPglu-600$\mu^{nuc}$). CFP and YFP fluorescence in COS-7 cells transformed with this construct was predominantly confined to the lumen of the nucleus (Fig. 2A,B), indicating successful nuclear targeting of the nanosensor, whereas FLIPglu-600$\mu$ carrying no targeting signal showed fluorescence distributed throughout the cell body, but excluded from the nucleus. Nuclear exclusion of FLIPglu-600$\mu$ is probably due to its relatively high molecular mass of 88 kDa. It is noteworthy that nuclei of COS-7 cells are polyploid and therefore much larger as compared to typical cells in native tissues. Weak cytosolic fluorescence in cells transfected with FLIPglu-600$\mu^{nuc}$ could only be detected when emission intensity images were overexposed and when the contrast ratio was reduced (Fig. 2C). Comparison of the emission intensity images of cells transfected with both nanosensors indicated that the fluorescent area of the cell can be reduced to ~30% by restricting the expression to the nucleus. Since the polyploid COS-7 nuclei have a relatively large size, the use of FLIPglu-600$\mu^{nuc}$ in native tissues should reduce the fluorescent fraction even more.

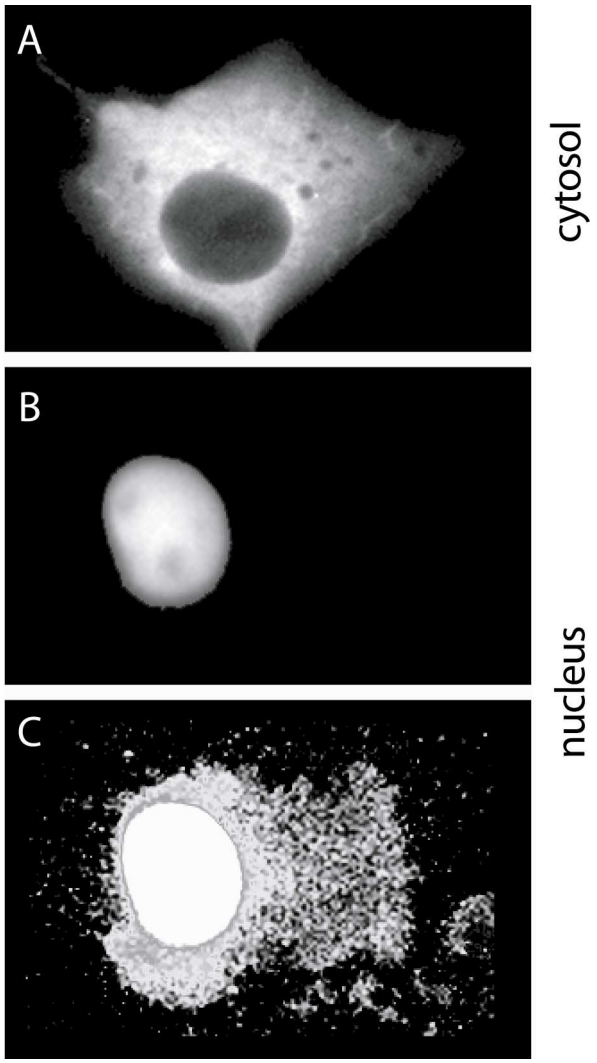


**Fig. 2.** (A) Emission intensity images following CFP excitation show that FLIPglu-600$\mu$'s expression in the cytosol of COS-7 cells is excluded from nuclei and lysosomes. (B) Expression of FLIPglu-600$\mu^{nuc}$ is restricted to the nucleus. (C) Reducing the contrast ratio and overexposing showed weak cytosolic fluorescence indicating that the fluorescent fraction is reduced to ~30% by using a nuclear nanosensor.

### Nuclear and Cytosolic Glucose Concentrations are coupled

Indirect determination of cytosolic glucose levels using a nuclear sensor requires free exchange of glucose between both compartments. Whereas passive transport of intermediate-sized macromolecules through the nuclear pore complex is regulated by nuclear calcium, small molecules (<1 kDa) and inorganic anions are supposed to freely diffuse even when nuclear calcium stores are depleted [12,13,15]. These results also indicate that the composition of the cytoplasm and the nucleoplasm will likely

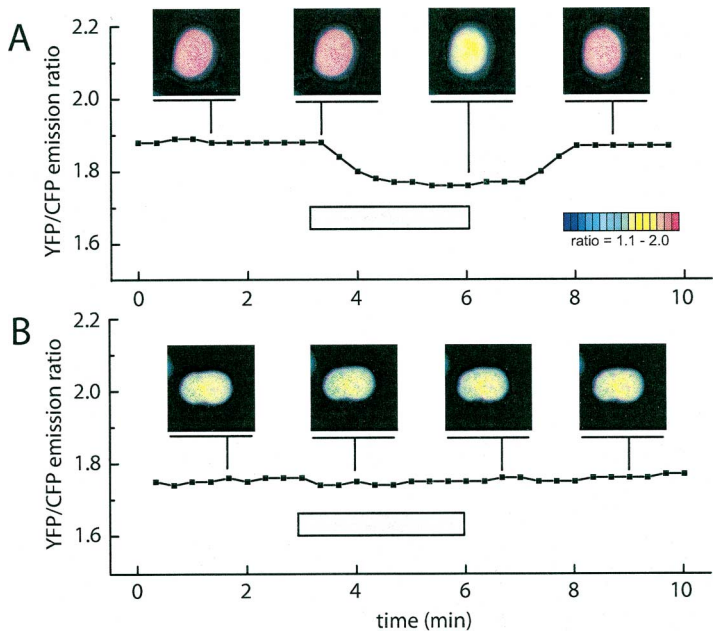


**Fig. 3.** Ratio images showing the YFP/CFP emission intensity ratio in COS-7 cells expressing FLIPglu-600$\mu^{nuc}$ and FLIPglu-170n$^{nuc}$ are pseudo-colored to demonstrate glucose dependent ratio changes. Red color represents high ratios, blue color low ratios. Integration over single nuclei was used to quantify the ratio change. Grey boxes indicate perfusion with 10 mM external glucose. (A) Perfusion with 10 mM external glucose following perfusion with glucose-free medium led to decreasing ratios in the nucleus of COS-7 cells expressing FLIPglu-600$\mu^{nuc}$ indicating increasing glucose levels in the nucleus. Upon withdrawing external glucose by perfusion with glucose-free medium the ratio was increasing indicating decreasing nuclear glucose levels. (B) The same perfusion pattern only induced very low ratio changes in COS-7 cells expressing high-affinity FLIPglu-170$^{nuc}$.

differ, potentially affecting the nanosensor's dynamic conformational changes [7]. To test whether cytosolic and nuclear concentrations are coupled and to show that FRET changes of FLIPglu-600$\mu^{nuc}$ are caused by altered nuclear glucose levels, FLIPglu-600$\mu^{nuc}$ and high-affinity FLIPglu-170n$^{nuc}$ were expressed in the nuclei of COS-7 cells. Due to its high-affinity of 170 nM, FLIPglu-170n$^{nuc}$ is saturated at concentrations that are in the detection range of FLIPglu-600$\mu^{nuc}$ and therefore should display a different pattern of ratio changes upon perfusion with external glucose. FRET may be used as a measure of intracellular glucose levels, under the assumption that *in vivo* ratio changes reflect the same parameters as the *in vitro* characteristics. FRET was determined *in vivo* using a fluorescence microscope and exciting CFP at 436 nm followed by simultaneous acquisition of CFP and YFP emission intensities using the DualView device and a digital camera. Ratio images were calculated on a pixel-by-pixel basis. For quantification, ratios were integrated over the area of single nuclei and displayed as a function of time. The growth medium was replaced by glucose-free medium before each measurement. Following perfusion with 10 mM external glucose the emission intensity ratio for cells expressing FLIPglu-600$\mu^{nuc}$ decreased, indicating rising nuclear glucose levels (Fig. 3A). Upon withdrawing external glucose by perfusion with glucose-free medium the ratio increased to its starting value, indicating decreasing nuclear glucose levels. Similar results were obtained for COS-7 cells expressing cytosolic FLIPglu-600$\mu$ [7], suggesting that nuclear and cytosolic glucose concentrations are coupled.

Perfusion of cells expressing FLIPglu-170n$^{nuc}$ with glucose-free medium followed by 10 mM external glucose did not cause significant ratio changes (Fig. 3B); only in some cases very small ratio changes were observed in the range of baseline fluctuations. To determine cytosolic glucose levels reliably in the absence of external supply, a new glucose-nanosensor with a detection range between those of FLIPglu-170n$^{nuc}$ and FLIPglu-600$\mu^{nuc}$ needs to be engineered.

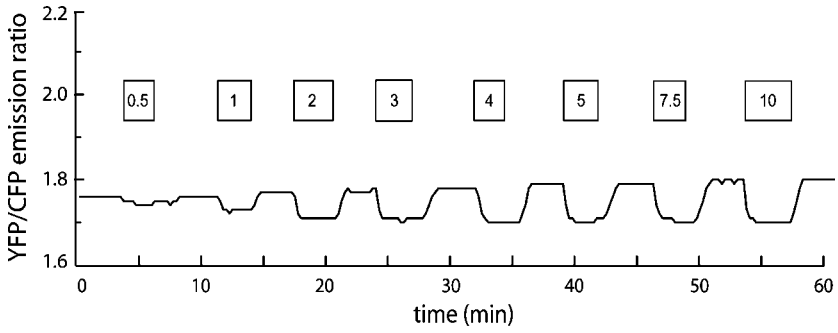


**Fig. 4.** Ratio change of a single cell expressing FLIPglu-600$\mu^{nuc}$ perfused with increasing external glucose concentrations. Boxes indicate external glucose concentrations (mM) during continuous perfusion with DMEM. The delta ratios increased with external supply following a saturation curve.

## Nuclear and Cytosolic Glucose Concentrations are both ~50% of External Supply

To determine cytosolic and nuclear glucose levels, COS-7 cells expressing FLIPglu-600$\mu^{nuc}$ were perfused with gradually increasing concentrations of external glucose (Fig. 4). After a constant ratio was reached, glucose was withdrawn by perfusion with glucose-free medium. Gradual stepwise elevation of external glucose between 0.5 and 10 mM led to increasing and reversible ratio changes. Ratio changes (delta ratio) averaged over 6 cells followed a hyperbolic curve, reflecting saturation of FLIPglu-600$\mu^{nuc}$ with increasing external supply. Similar results were obtained for cytosolic FLIPglu-600$\mu$ [7]. To normalize the ratio changes, the minimum ratio change in the absence of glucose ($\Delta R_{min}$) and maximum ratio change ($\Delta R_{max}$) at glucose saturation were determined using non-linear regression (Eqs. (1) and (2)). The normalized ratio changes (saturation) were similar for both sensors (Fig. 5A). Using the $K_d$ as determined *in vitro*, normalized ratio changes were transformed into internal glucose concentrations (Eq. (3)), assuming that the ratio changes are unaffected by differences in the two intracellular environments. Although the concentration of the nanosensors may be higher in the nucleus, saturation of FLIPglu-170n$^{nuc}$ indicates that the sensor concentration is below the concentration of its substrate. Thus, despite potential variation in sensor levels it seems adequate to compare glucose levels between experiments using cytosolic and nuclear sensors. Under these boundary conditions, results from the two experimental sets can be compared directly. Both nuclear and cytosolic glucose levels increased with external supply, but remained at ~50% relative to the external medium indicating that glucose can freely diffuse through the nuclear pore (Fig. 5B). However, due to decreased sensitivity of the nanosensors close to saturation, determination of high internal glucose levels are less reliable than measuring low internal levels. Thus, expanding the range for quantification by engineering sensors with lower affinity and higher maximum ratio changes will increase the performance of the novel nanosensor technology.

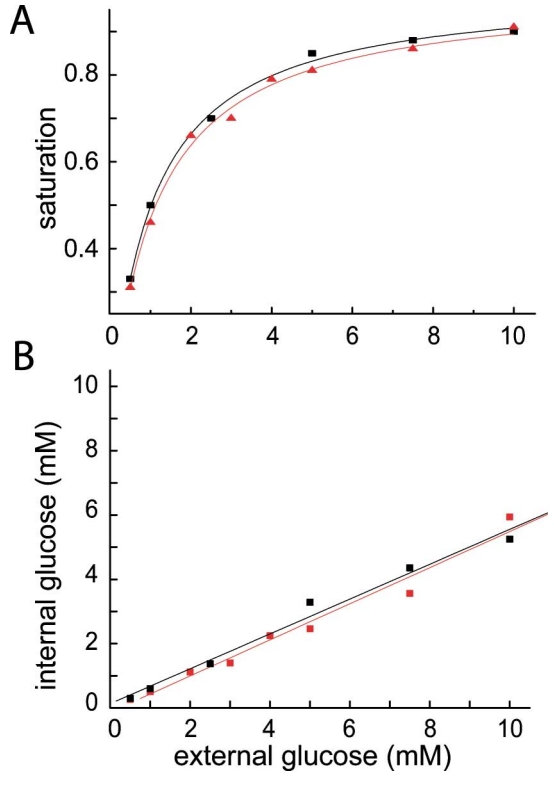


**Fig. 5.** Averaged delta ratios from cells expressing FLIPglu-600$\mu$ (■, $n = 5$) and FLIPglu-600$\mu^{nuc}$ (▲, $n = 6$) were normalized. (A) Normalized ratio changes (saturation) were similar for both nanosensors. (B) Cytosolic (■) and nuclear (■) glucose concentrations increased with external supply but remained at ~50% of external levels as demonstrated by linear regression.

In summary we could show that restriction of fluorescence to the nucleus allowed us to acquire emission intensities in individual cells even deep in native tissues. FLIPglu-600$\mu^{nuc}$ expression was successfully targeted to the nucleus, where it was used to monitor dynamic glucose changes indicating that glucose can freely diffuse through the nuclear pore complex. Nuclear and cytosolic levels were each shown to be $\sim$50% of external supply. Together, these results indicate that indirect measurement of cytosolic glucose levels deep in tissues will be possible using nuclear sensors. Thus in future experiments, nuclear localized nanosensors will be used to image glucose levels in plant and animal tissues.

## REFERENCES


1. K. Jungermann and T. Kietzmann (1996). Zonation of parenchymal and nonparenchymal metabolism in liver. *Annu. Rev. Nutr.* **16**, 179–203.
2. K. Jungermann (1983). Functional significance of hepatocyte heterogeneity for glycolysis and gluconeogenesis. *Pharmacol. Biochem. Behav.* **18**(Suppl. 1), 409–414.
3. K. Jungermann and N. Katz (1989). Functional specialization of different hepatocyte populations. *Physiol. Rev.* **69**, 708–764.
4. G. M. Lawrence, *et al*. (1986). The compartmentation of glycolytic and gluconeogenic enzymes in rat kidney and liver and its significance to renal and hepatic metabolism. *Histochem. J.* **18**, 45–53.
5. B. Roeckl (1949). Nachweis eines Konzentrationshubs zwischen Palisadenzellen und Siebröhren. *Planta* **36**, 530–550.
6. M. Fehr, *et al*. (2002). Visualization of maltose uptake in living yeast cells by fluorescent nanosensors. *Proc. Natl. Acad. Sci. U.S.A.* **99**, 9846–9851.
7. M. Fehr, *et al*. (2003). *In vivo* imaging of the dynamics of glucose uptake in the cytosol of COS-7 cells by fluorescent nanosensors. *J. Biol. Chem.* **278**, 19127–19133.
8. I. Lager, *et al*. (2003). Development of a fluorescent nanosensor for ribose. *FEBS Lett.* **553**, 85–89.
9. F. A. Quiocho and P. S. Ledvina (1996). Atomic structure and specificity of bacterial periplasmic receptors for active transport and chemotaxis: Variation of common themes. *Mol. Microbiol.* **20**, 17–25.
10. R. M. de Lorimier, *et al*. (2002). Construction of a fluorescent biosensor family. *Protein Sci.* **11**, 2655–2675.
11. G. Gilardi, *et al*. (1994). Engineering the maltose binding protein for reagentless fluorescence sensing. *Anal. Chem.* **66**, 3840–3847.
12. C. Perez-Terzic, *et al*. (1996). Conformational states of the nuclear pore complex induced by depletion of nuclear Ca2+ stores. *Science* **273**, 1875–1877.
13. L. Stehno-Bittel, *et al*. (1995). Diffusion across the nuclear envelope inhibited by depletion of the nuclear Ca2+ store. *Science* **270**, 1835–1838.
14. Cutler *et al*. (2000). Random GFP::cDNA fusions enable visualization of subcellular structures in cells of Arabidopsis at a high frequency. *Proc. Natl. Acad. Sci. U.S.A.* **97**, 3718–3723.
15. U. F. Greber and L. Gerace (1995). Depletion of calcium from the lumen of endoplasmic reticulum reversibly inhibits passive diffusion and signal-mediated transport into the nucleus. *J. Cell. Biol.* **128**, 5–14.